# Monazite–huttonite solid-solutions from the Vico Volcanic Complex, Latium, Italy

GIANCARLO DELLA VENTURA, ANNIBALE MOTTANA

Dipartimento di Scienze Geologiche, Università di Roma Tre, Via Ostiense 169, I-00154 Roma, Italy

GIAN CARLO PARODI*

Museo di Mineralogia, Università di Roma "La Sapienza", Piazzale Aldo Moro 5, I-00185 Roma, Italy

MATI RAUDSEPP

Department of Geological Sciences, University of British Columbia, 6339 Stores Road, Vancouver, B.C. V6T 1Z4, Canada

FABIO BELLATRECCIA, ENRICO CAPRILLI, PAOLO ROSSI AND SALVATORE FIORI

Dipartimento di Scienze della Terra, Università di Roma "La Sapienza", Piazzale Aldo Moro 5, I-00185 Roma, Italy

## Abstract

The crystal-chemical relationships occurring within a single grain of monazite-(Ce) from Vetralla, Vico Volcanic Complex, north of Rome, are outlined. The sample is from a miarolitic cavity in a holocrystalline ejectum consisting of K-feldspar plus minor plagioclase, mica and Fe-oxides, collected from a pyroclastic explosive level. The Gandolfi film (Cu-$K\alpha$ radiation) can be indexed in space group $P2_1/n$ with $a = 6.816(4)$; $b = 6.976(4)$; $c = 6.471(3)$ Å; $\beta = 103.63(3)°$; V = 299.0(6) Å$^3$. Electron-probe microanalyses plot within the field of monazite along the huttonite–monazite edge of the huttonite–monazite–brabantite triangle. Despite patchy and irregular zoning, the grain shows a clear enrichment towards pure monazite at the outer rim. A constant Th:Si ratio of 1:1 indicates the existence of a simple solid-solution between huttonite and monazite. The substitution can be written as $Th^{4+} + Si^{4+} \rightarrow REE^{3+} + P^{5+}$ without requiring any electrostatic compensation by divalent cations, or by anionic groups. The *REE* distribution pattern is compatible with that of monazites from syenitic rocks.

KEYWORDS: monazite, huttonite, Latium, Italy, cell parameters, crystal-chemistry.

## Introduction

MONAZITE is the general name for *REE*-bearing phosphate minerals, *REE*[$PO_4$], which according to the dominating *RE* element (Levinson's rule), can either be the species monazite-(Ce) with Ce > La, Nd (the original monazite), monazite-(La) with La > Ce, Nd, or monazite-(Nd) with Nd > La and Ce. Monazite-(Ce) is common in pegmatites associated with granites and syenites, and in metamorphic rocks and vein deposits. In addition, it occurs as a minor accessory phase in granites, alkaline rocks, and carbonatites. Occurrences of monazite-(Ce) as a metasomatic phase in dolomitic marbles (von Knorring and Clifford, 1960), or as *in situ* recrystallization of detrital grains have also been reported (Read *et al.*, 1987). Common monazite (monazite-(Ce)) displays extensive solid-solutions whereby *REE* are substituted by Th (plus U), while

* Present address: Museum National d'Histoire Naturelle, Laboratoire de Minéralogie, 61, rue Buffon, 75005 Paris, France.

*Mineralogical Magazine, October 1996, Vol. 60, pp. 751 758*

P is substituted by Si. These substitutions lead to the isostructural species huttonite, $Th[SiO_4]$ (Pabst and Hutton, 1951), through to the intermediate phase cheralite, $(Ce,Th,Fe,Ca)[(P,Si)O_4]$ (Bowie and Horne, 1953), and the as yet unaccepted species 'cerphosphorhuttonite', $(Th,Ce,Fe,U)[(Si,P)O_4]$ (Pavlenko *et al.*, 1965).

In Italy, monazites are well known from alpine occurrences both in pegmatites and as fissure minerals (Mannucci *et al.*, 1986; Demartin *et al.*, 1991). The alpine fissures of Glogstafel and Cervandone, in Val Formazza, are the type localities of monazite-(Nd) (Graeser and Schwander, 1987) and paraniite-(Y) (Demartin *et al.*, 1994). The Piona pegmatite on Lake Como yielded monazite-(Ce) with exceptionally high U and Th contents (Gramaccioli and Segalstad, 1978).

Since monazite is relatively resistant to weathering, it is widespread as a detrital mineral in placer deposits and beach sands. Monazite was first described in Latium from such deposits at Nettuno beach (Gottardi, 1952), occurring as grains associated with other Th and *REE*-bearing minerals, and the new mineral perrierite (Bonatti and Gottardi, 1950). The Nettuno sands are derived from disaggregation of pyroclastic rocks in the Alban Hills, in the volcanic Roman Perpotassic Province nearby to the west. Since then, monazite has not been found in primary settings in Latian rocks, despite the careful search of mineralogists and mineral collectors.

This paper reports the first *in situ* finding of monazite in Latium, from an ejectum within pyroclastic rocks belonging to another volcanic centre in the Roman Perpotassic Province of central Italy. This new occurrence is genetically linked to the Alban Hills, but several kilometres to the north in the Vico Volcanic Complex.

## Occurrence

The monazite-(Ce) sample was collected from a loose fragment of ejectum at Vetralla, Viterbo Province. Known locally known as 'sanidinite', the ejectum is a peculiar rock of syenitic appearance. Although the area has outcrops of the pyroclastic 'ignimbrite A' horizon (Locardi, 1965), the ejectum has no evident stratigraphic relationship with the bedrock.

In thin section, the ejectum shows a subhedral equigranular texture consisting of dominant K-feldspar, minor plagioclase, mica and Fe-oxides. K-feldspar crystals vary in composition from sodian sanidine ($Or_{85}Ab_{14}An_1$) at the core to anorthoclase ($Or_{56}Na_{42}An_2$) at the rim. Plagioclase ranges from oligoclase ($Ab_{71}An_{25}Or_4$) to almost pure albite ($Ab_{99}Or_1$), and is particularly abundant (and most Na-rich) around the vugs where monazite occurs. Two types of mica can be identified optically: (1) early-formed and strongly pleochroic with irregular zoning, corrosion and reaction rims, and with segregation of tiny opaque oxides along the cleavage planes; (2) a second generation of mica flakes, colourless or with extremely weak yellowish pleochroism restricted to some central patches in the interstices between the early-formed feldspars. The first type of mica is biotitic in composition, the second one is close to F-rich phlogopite. Both show irregular zoning.

Tourmaline and zircon are the only identified accessory phases. Zircon is scattered at random throughout the groundmass, whereas tourmaline is a late phase restricted to vugs. It is strongly pleochroic from a dark brown to a yellow brown, and forms fan-shaped crystals radiating from the albite walls of the vug.

Monazite occurs inside the vugs and other cavities as light-yellow, transparent, euhedral stubby crystals, up to 0.35 mm long. It is characteristically associated with Th-rich peprossiite-(Ce), $(Ce,La)Al_2B_3O_9$, a new *REE*-bearing borate recently described from the Sabatini volcanic district (Della Ventura *et al.*, 1993).

## Experimental methods

Monazite was found during a systematic qualitative SEM-EDS study of several unidentified crystals observed inside the holocrystalline ejecta of the Vico volcanics, but was later positively identified by X-ray diffraction using a Gandolfi camera. The XRD pattern was indexed in the space group $P2_1/n$, and cell parameters were computed by least-squares refinement (Table 1). Electron-probe microanalyses were carried out using a Cameca SX50 microprobe operating in the wavelength-dispersive mode. The analytical conditions and standards used are summarized in Table 2.

## Results

*Cell dimensions.* Table 1 compares the cell dimensions of the Vetralla monazite with those of other synthetic and natural monazite-type compounds. Although numerous cell dimensions of monazites of different compositions have been reported, no clear systematic relationship between individual cell edges and chemical composition (e.g. the Th content) has yet been observed (Kato, 1958) due to the complicated compositional variations possible in the structure. However, the cell volume varies linearly with composition. The cell volume *vs.* the cubed mean ionic radius of cations located in the *A* site are plotted for selected natural and synthetic monazites in Fig. 1. For simplicity, the *A*-site is

TABLE 1. Unit-cell data of the Vetralla monazite-(Ce) and other synthetic and natural monazite-type compounds

| | $a$(Å) | $b$(Å) | c(Å) | β(°) | V(Å$^3$) |
|---|---|---|---|---|---|
| Vetralla | 6.816(4) | 6.976(4) | 6.471(3) | 103.63(3) | 299.0(6) |
| Nettuno | 6.78(2) | 7.00(2) | 6.43(2) | 103.67(25) | 296 (3) |
| Piona | 6.68 | 6.96 | 6.48 | 103.90 | 296.8 |
| Th[SiO]$_4$ | 6.80(3) | 6.96(3) | 6.54(3) | 104.92(6) | 299.0 |
| La[PO]$_4$ | 6.89 | 7.05 | 6.48 | 104.57 | 304.6 |
| Ce[PO]$_4$ | 6.777 | 6.993 | 6.445 | 103.5 | 297.0 |
| Pr[PO]$_4$ | 6.75 | 6.94 | 6.40 | 103.35 | 292 |
| Nd[PO]$_4$ | 6.71 | 6.92 | 6.36 | 103.47 | 287 |

Vetralla: this work.
Nettuno: Gottardi (1952).
Piona: natural U-rich monazite, Gramaccioli and Segalstad (1978).
Th: natural huttonite, Pabst and Hutton (1951).
La: synthetic, Semenov (1963).
Ce: synthetic, Boatner *et al.* (1980).
Pr: synthetic, Mooney (1948).
Nd: synthetic, Mooney (1948).

assumed to be 8-coordinated. The trend for the synthetic $B^{3+}$[PO]$_4$ phosphates is close to linear, and indicates that pure monazite-type compounds obey Vegard's law. In contrast, the points for natural monazites are scattered, but the trend is generally linear (shaded areas in Fig. 1).

Natural monazites deviate from the strictly linear trend for two reasons: (i) the complex coupled substitutions of cations at the *A* (and *B*) site; and (ii) most monazites are slightly metamict and thus have a 'lattice distension' with cell parameters slightly larger than the expected ones (Kato, 1958). The Vetralla monazite is close to the trend of the synthetic samples because it is neither metamict nor has complex substitutions with a composition close to that of (Ce,La)-phosphate.

*Electron-probe microanalyses.* Back-scattered electron (BSE) images show irregular and patchy

TABLE 2. Conditions and standards for microprobe analyses

| Element | Line | Standard | Crystal | Counting time: (s) std/sample |
|---|---|---|---|---|
| P | Kα | Apatite | PET | 20/20 |
| Si | Kα | Diopside | TAP | 20/20 |
| Ca | Kα | Diopside | PET | 20/20 |
| Th | Mα | syn. $ThO_2$ glass | PET | 20/20 |
| La | Lα | Drake glass | PET | 40/40 |
| Ce | Lα | syn. $CeO_2$ glass | PET | 20/40 |
| Pr | Lβ | D+W* | PET | 40/40 |
| Nd | Lα | D+W | LIF | 40/40 |
| Sm | Lβ | D+W | LIF | 40/40 |
| Gd | Lα | D+W | LIF | 40/40 |

Accelerating voltage: 15 kV
Beam current: 20 nA
Spot size: 5 μm

* Drake and Weill (1972)

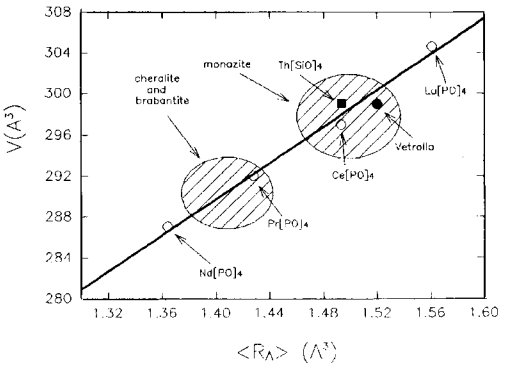


FIG. 1. Unit cell volume as a function of the cubed mean cation radius at the *A* site for monazite-type compounds.

zoning of the single grain studied, except for very fine, regular lamella parallel to the preserved crystal faces (Fig. 2). To characterize the wide variation in chemical composition, analyses were done in each zone; individual lamellae in the regularly zoned part could not be resolved. Analyses are given in Table 3, while the locations of the analysed points are shown in Fig. 2. The analysed grain is highly inhomogeneous (Table 3). The average composition of the grain may be classified as monazite-(Ce), since all points have Ce > La ≫ Nd > Gd = Pr > Sm. There is, however, significant substitution of $Si^{4+}$ for $P^{5+}$ at the *B* site, which is compensated for by substitution of $Th^{4+}$ for $REE^{3+}$ at the *A* site. The $SiO_2$ content increases monotonically and is inversely correlated with decreasing $P_2O_5$ content (Table 3). There is a parallel increase in $ThO_2$, a decrease in the total *REE* (notably $La_2O_3$) and Ca content, but the $Gd_2O_3$ content remains significant and constant. Thus the grain shows a continuous compositional trend from near end-member monazite-(Ce,La) (M18-7, Table 3) to about 30% huttonite component (M18-4, Table 3). Note that the zoned exterior part of the crystal is closest to end-member monazite composition (M18-6 and M18-7, Table 3). Further-

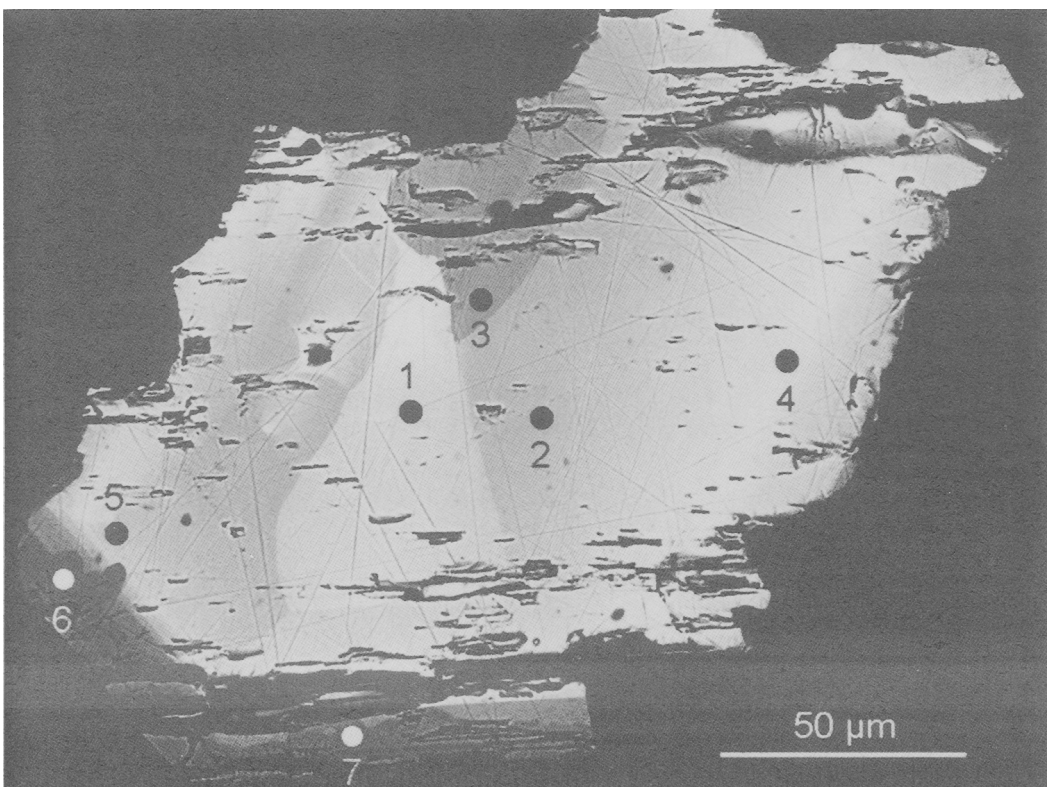


FIG. 2. BSE picture of the analyzed monazite-(Ce) grain showing patchy zoning. The darkness of the different grey tones is proportional to Z (atomic number). The location of the point-analyses is shown.

TABLE 3. Electron-probe microanalyses and crystal-chemical formulae for the Vetralla monazite-(Ce)

| | M18-4 | M18-1 | M18-5 | M18-2 | M18-3 | M18-6 | M18-7 |
|---|---|---|---|---|---|---|---|
| $P_2O_5$ | 19.12 | 19.97 | 21.07 | 21.09 | 23.45 | 28.23 | 29.88 |
| $SiO_2$ | 6.29 | 5.86 | 5.32 | 5.01 | 3.79 | 1.03 | 0.11 |
| CaO | 0.07 | 0.16 | 0.12 | 0.17 | 0.16 | 0.70 | 0.99 |
| $ThO_2$ | 27.12 | 25.31 | 23.80 | 21.06 | 15.39 | 6.62 | 5.12 |
| $La_2O_3$ | 15.06 | 15.00 | 16.14 | 16.82 | 18.34 | 24.08 | 26.62 |
| $Ce_2O_3$ | 24.39 | 25.62 | 25.91 | 27.18 | 29.96 | 31.68 | 30.79 |
| $Pr_2O_3$ | 1.59 | 1.93 | 1.74 | 1.84 | 2.15 | 1.77 | 1.46 |
| $Nd_2O_3$ | 3.91 | 4.26 | 4.45 | 4.24 | 4.49 | 3.90 | 3.32 |
| $Sm_2O_3$ | 0.30 | 0.21 | 0.33 | 0.23 | 0.16 | 0.11 | 0.24 |
| $Gd_2O_3$ | 2.24 | 2.20 | 2.22 | 2.38 | 2.43 | 3.00 | 2.73 |
| Total | 100.09 | 100.52 | 101.10 | 100.02 | 100.32 | 101.12 | 101.26 |
| Number of cations on the basis of 4 oxygens | | | | | | | |
| $P^{5+}$ | 0.71 | 0.73 | 0.76 | 0.77 | 0.83 | 0.95 | 0.99 |
| $Si^{4+}$ | 0.28 | 0.25 | 0.23 | 0.22 | 0.16 | 0.04 | 0.00 |
| Sum B | 0.98 | 0.98 | 0.99 | 0.98 | 0.99 | 0.99 | 0.99 |
| $Ca^{2+}$ | 0.00 | 0.01 | 0.01 | 0.01 | 0.01 | 0.03 | 0.04 |
| $Th^{4+}$ | 0.27 | 0.25 | 0.23 | 0.21 | 0.15 | 0.06 | 0.05 |
| $La^{3+}$ | 0.24 | 0.24 | 0.25 | 0.27 | 0.28 | 0.35 | 0.38 |
| $Ce^{3+}$ | 0.39 | 0.41 | 0.40 | 0.43 | 0.46 | 0.46 | 0.44 |
| $Pr^{3+}$ | 0.03 | 0.03 | 0.03 | 0.03 | 0.03 | 0.03 | 0.02 |
| $Nd^{3+}$ | 0.06 | 0.07 | 0.07 | 0.07 | 0.07 | 0.06 | 0.05 |
| $Sm^{3+}$ | 0.01 | 0.00 | 0.01 | 0.00 | 0.00 | 0.00 | 0.00 |
| $Gd^{3+}$ | 0.03 | 0.03 | 0.03 | 0.03 | 0.03 | 0.04 | 0.04 |
| Sum A | 1.03 | 1.03 | 1.02 | 1.04 | 1.03 | 1.02 | 1.01 |

more, although Gd has rarely been detected in other Latian minerals, it is present here in significant amounts (2.2–3.0% oxide). Thus the Vico monazite is chemically different from all other monazites described previously from Italy (Mannucci *et al.*, 1986; Demartin *et al.*, 1991).

## Discussion

Monazite-group minerals have space group $P2_1/n$ and general formula $ABO_4$, and can be conveniently classified in the ternary system monazite (Mo), $REE[PO]_4$ – brabantite (Br), $CaTh[PO_4]$ – huttonite (Hu), $Th[PO_4]$ (Bowie and Horne, 1953).

The structure of the monazite group may be described as a three-dimensional network of edge-sharing $AO_9$ polyhedra linked by $BO_4$ tetrahedra (Ueda, 1967). Cheralite (Finney and Rao, 1967) and huttonite (Taylor and Ewing, 1978) are isostructural with monazite, but the details of the various structures differ slightly. This basic stucture of the group resembles that of zircon and xenotime, in that chains of alternating $BO_4$ and $AO_9$ polyhedra extend parallel to the *c*-axis. An even greater similarity is obtained if the site centred by the *A* cation is taken as being 8-fold rather than 9-fold coordinated. In this case, it is assumed that the oxygen at distance > 3.3 Å is too far to be included in the coordination polyhedron and the average <*A*–O> bond distance is 2.45 Å, i.e. similar to that of xenotime (2.42 Å). This assumption implies unbonded space in the structure, however, and this may be the reason for certain substitutions suggested that defy the simple coupled substitution outlined above, and other less simple substitutions which also involve the *A* and *B* sites, such as $A^{2+}B^{6+}$, $A^{3+}B^{5+}$ and $A^{4+}B^{4+}$.

The substitution relating huttonite to monazite in our grain is a simple coupled substitution of P by Si at the *B* site, balanced by Th-*REE* substitution in the *A* site: $Th^{4+}+Si^{4+} = REE^{3+}+P^{5+}$ (Fig. 3), with no or negligeable brabantite component, as indicated by its very low Ca content (Table 3).

The Th:Si ratio being constantly 1:1 also supports the existence of the straightforward solid-solution along the binary join $REE[PO_4]$–$Th[SiO_4]$, as suggested by Starynkevitch (1922). Later confirmation by Bowie and Horne (1953) and Pavlenko *et al.* (1965) did not enjoy wide acceptance, possibly

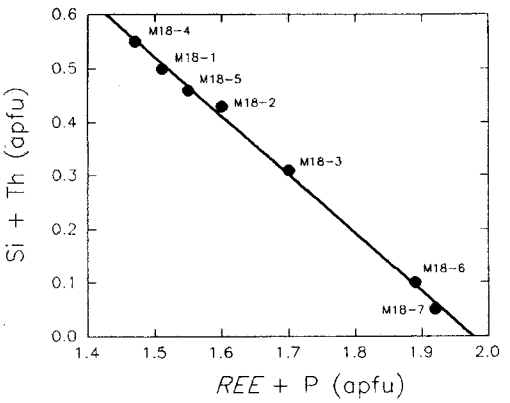


FIG. 3. $Th^{4+} + Si^{4+}$ *vs.* $REE^{3+} + P^{5+}$ relationship in the Vetralla monazite-(Ce) grain.

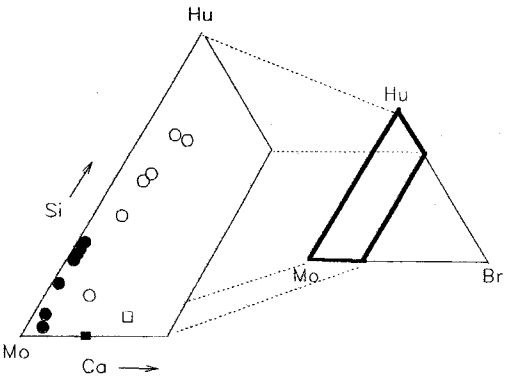


FIG. 4. Plot of the point analyses onto the Hu (huttonite) – Mo (monazite) – Br (brabantite) triangle. Filled circles: this work; open circles: data from Kucha (1980); filled square: Piona monazite (Gramaccioli and Segalstad 1978); open square: cheralite (Bowie and Horne, 1953).

because they were based on averaged wet chemical analyses with no indication of the sample homogeneity. Our data leave no doubts.

More recently, the continuity of the monazite–huttonite series was endorsed by Kucha (1980) with a microprobe study of six different crystals from Bogatynia, Poland, having compositions extending from $Mo_{88}Hu_{12}$ to $Mo_{30}Hu_{70}$. However, Kucha (1980) argued that the huttonite–monazite series cannot be explained solely by the simple coupled substitution $Th^{4+} + Si^{4+} \rightarrow RE^{3+} + P^{5+}$, and concluded that there must be an electrostatic compensation by the concomitant entrance of Ca,F and $(OH)_4$, leading to a formula for intermediate members of the series of $(RE,Th,M^{2+},U)$-$[PO_4,SiO_4,OH,F]$, similar to cheralite (Bowie and Horne, 1953).

This inference seems not to hold true for our sample. In the present case the linear variation is observed inside the same grain, and extends from $Mo_{100}$ to $Mo_{70}Hu_{30}$ (Fig. 4). No OH was determined either by Kucha (1980) or in this study. Kucha (1980) inferred OH to be present up to 5.1 (and $H_2O$ up to 0.6) wt.% from high deficits in the analytical sum. In our sample, we can exclude OH and $H_2O$ since our analyses (Table 3) total nearly 100 wt.%, and also because the sums of atoms p.f.u. (on the basis of 4 oxygens) are systematically higher than 2. Fluorine was sought in our samples but not found. The same is the case of divalent cations, which are virtually absent.

These observations indicate that the simple substitution $Th^{4+} + Si^{4+} \rightarrow RE^{3+} + P^{5+}$ occurred in our sample without any electrostatic compensation by Ca, F or OH. This is also confirmed by the unit-cell data. The points representing pure synthetic $Ce(PO)_4$ and $Th(SiO)_4$ in Fig. 1 are very similar since the decrease in mean ionic radius at the *A*-site induced by the substitution of Ce (1.143 Å: Shannon, 1976) by Th (1.05 Å) is exactly compensated by the increase in the mean ionic radius at the *B*-site due to the substitution of Si (0.26 Å) for P (0.17 Å). This results in the huttonite component having an insignificant effect on the cell volume for monazite–huttonite solid-solutions, and does not displace them from the linear trend. This would not have been the case, had either Ca (1.12 Å) or OH, F (1.33 Å) been present.

The *REE* distribution in our sample deserves a comment. All monazite-type minerals have invariably high ceric *REE* distribution (Pabst and Hutton, 1951; Murata *et al.*, 1953, 1958; Lee and Bastron, 1967; Fleischer and Altschuler, 1969; Bowles *et al.*, 1980; Fleischer and Rosenblum, 1990). This is also the case for the monazites from Latium (Gottardi, 1952; this work) and all the Alpine monazites (Mannucci *et al.*, 1986; Demartin *et al.*, 1991), including the 'anomalous' sample from Piona (Gramaccioli and Segalstad, 1978).

It is well known that the *REE* distribution of monazites can be confidently correlated with their geological environment of formation (Murata *et al.*, 1953, 1957, 1958; Vainshtein *et al.*, 1956; Lee and Bastron, 1967; Fleischer and Altschuler, 1969). The *REE* distributions for our two extreme compositions (M18-1, M18-7) are shown in Fig. 5 with *REE* averages reported in the mineralogical literature for monazites occurring in granitic and alkaline rocks. The Vico sample trend follows the general trend of

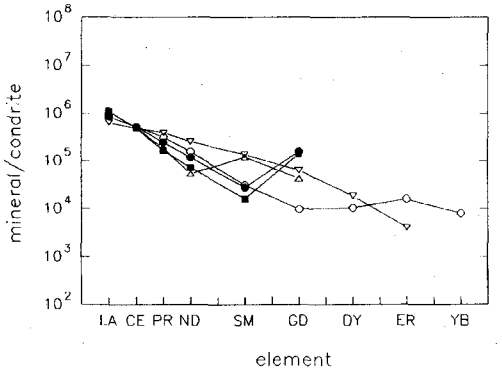


FIG. 5. Chondrite-normalized *REE* distribution of average monazite from different geological environments in comparison with our points M18-1 and M18-7. Filled circle: M18-1; filled square: M18-7; open circles: syenitic rocks; triangle down: granitic rocks; triangle up: Piona monazite.

monazites from alkaline rocks. A strong departure from the trend is observed only in the Gd content (Fig. 5) which is unusually high compared with recent microprobe determinations for alpine monazites (Mannucci *et al.*, 1986; Demartin *et al.*, 1991), but is not exceptional in comparison with monazites occurring in certain pegmatites (Petruk and Owens, 1975; Hanson *et al.*, 1992).

The strong compositional difference between the Vico *in situ* and the Nettuno detrital manazite, which is enriched in heavy *REE* and Y ($Y_2O_3$ = 4.51 wt.%: Gottardi, 1952) might be an analytical artifact. The Alban Hills holocrystalline ejecta, probably the host rocks of the Nettuno monazite, are strongly depleted in heavy *REE*, and completely lack yttrium (Federico *et al.*, 1994).

## Acknowledgements

This work was supported by the Commissione Musei Naturalistici, Accademia Nazionale dei Lincei, and by an operating grant to MR from the Natural Sciences and Engineering Research Council of Canada. The manuscript benefited by the constructive criticism of J.F.W. Bowles and an anonymous referee.

## References

Boatner, L.A., Beall, G.W., Abraham, M.M., Finch, C.B., Huray, P.G. and Rappaz, M. (1980) Monazite and other lanthanide orthophosphates as alternate actinide waste forms. In *Scientific basis for nuclear waste management*, **2** (C.J.M. Northrup, Jr., Ed.), Plenum Press, New York.

Bonatti, S. and Gottardi, G. (1950) Perrierite, nuovo minerale ritrovato nella sabbia di Nettuno (Roma). *Atti Acc. Naz. Lincei, Rend. cl. Sc. Mat. Fis. Nat.*, s. **8**, **9**, 361–8.

Bowie, S.H.U. and Horne, J.E.T. (1953) Cheralite, a new mineral of the monazite group. *Mineral. Mag.*, **30**, 93–9.

Bowles, J.F.W., Jobbins, E.A. and Young, B.R. (1980) A re-examination of cheralite. *Mineral. Mag.*, **43**, 885–8.

Della Ventura, G., Parodi, G.C., Mottana, A. and Chaussidon, M. (1993) Peprossiite-(Ce), a new mineral from Campagnano (Italy): the first anhydrous rare-earth-element borate. *Eur. J. Mineral.*, **5**, 53–8.

Demartin, F., Pilati, T., Diella, V., Donzelli, S. and Gramaccioli, C.M. (1991) Alpine monazite: further data. *Canad. Mineral.*, **29**, 61–67.

Demartin, F., Gramaccioli, C.M. and Pilati, T. (1994) Paraniite-(Y), a new tungstate arsenate mineral from alpine fissures. *Schweiz. Mineral. Petrol. Mitt.*, **74**, 155–160.

Drake, M.J. and Weill, D.F. (1972) New rare earth element standards for electron microprobe. *Chem. Geol.*, **10**, 179–81.

Federico, M., Peccerillo, A., Barbieri, M. and Wu, T.W. (1994) Mineralogical and geochemical study of granular xenoliths from the Alban Hills volcano, Central Italy; bearing on evolutionary processes in potassic magma chambers. *Contrib. Mineral. Petrol.*, **115**, 384–401.

Finney, J.J. and Rao, N.N. (1967) The crystal structure of cheralite. *Amer. Mineral.*, **52**, 13–19.

Fleischer, M. and Altschuler, Z.S. (1969) The relationship of the rare-earth composition of minerals to geological environment. *Geochim. Cosmochim. Acta*, **33**, 725–32.

Fleischer, M. and Rosenblum, S. (1990) The distribution of lanthanides and yttrium in the minerals of the monazite family. *U.S. Geol. Surv., Open-File Repts.*

Gottardi, G. (1952) La sabbia di Nettuno (Roma). *Atti Soc. Tosc. Sc. Nat. Mem.*, **59**, 36–62.

Graeser, S. and Schwander, H. (1987) Gasparite-(Ce) and monazite-(Nd): two new minerals of the monazite group from the Alps. *Schweiz. Mineral. Petrol. Mitt.*, **67**, 103–113.

Gramaccioli, C.M. and Segalstad, T.V. (1978) A uranium- and thorium-rich monazite from a south-alpine pegmatite at Piona, Italy. *Amer. Mineral.*, **63**, 757–61.

Hanson, S.L., Simmons, W.B., Webber, K.L. and Falster A.U. (1992) Rare-earth-element mineralogy of granitic pegmatites in the Trout Creek Pass district, Chaffee county, Colorado. *Canad. Mineral.*, **30**, 673–86.

Kato, T. (1958) A study on monazite from the Ebisu Mine, Gifu Prefecture. *Mineral. J.*, **4**, 224–35.

Kucha, H. (1980) Continuity in the monazite-huttonite series. *Mineral. Mag.*, **43**, 1031–4.

Lee, D.E. and Bastron, H. (1967) Fractionation of rare-earth elements in allanite and monazite as related to geology of the Mt. Wheeler mine area, Nevada. *Geochim. Cosmochim. Acta*, **31**, 339–56.

Locardi, E. (1965) Tipi di ignimbriti di magmi mediterranei: il vulcano di Vico. *Atti Soc. Tosc. Sc. Nat.*, **45**, 55–173.

Mannucci, G., Diella, V., Gramaccioli, C.M. and Pilati, T. (1986) A comparative study of some pegmatitic and fissure monazite from the Alps. *Canad. Mineral.*, **24**, 469–74.

Mooney, R.C.L. (1948) Crystal structures of a series of rare earth phosphates. *J. Chem. Phys.*, **16**, 1003.

Murata, K.J., Rose, H.J.jr. and Carron, M.K. (1953) Systematic variation of rare earths in monazite. *Geochim. Cosmochim. Acta,* **4**, 292–300.

Murata, K.J., Rose, H.J. jr., Carron, M.K. and Glass, J.J. (1957) Systematic variation of rare-earth elements in cerium-earth minerals. *Geochim. Cosmochim. Acta*, **11**, 141–61.

Murata, K.J., Dutra, C.V., Teixeira da Costa, M. and Branco, J.J.R. (1958) Composition of monazites from pegmatites in eastern Minas Gerais, Brasil. *Geochim. Cosmochim. Acta*, **16**, 1–14.

Pabst, A. and Hutton, C.O. (1951) Huttonite, a new monoclinic thorium silicate. *Amer. Mineral.*, **36**, 60–9.

Pavlenko, A.S., Orlova, L.P. and Akhmanova, M.V. (1965) Cerphosphorhuttonite, a monazite-group mineral. *Trudy Mineral. Muzeya Akad. Nauk SSSR*, **16**, 166–74 (in Russian).

Petruk, W. and Owens, D. (1975) Monazite from the Mount Pleasant deposit, New Brunswick. *Canad. Mineral.*, **13**, 298–9.

Read, D., Cooper, D.C. and McArthur, J.M. (1987) The composition and distribution of nodular monazite in the Lower Palaeozoic rocks of Great Britain. *Mineral. Mag.*, **51**, 271–80.

Semenov, E.I. (1963) Mineralogy of the rare earths. *USSR Academy of Sciences*, Moskow (in Russian).

Shannon, R.D. (1976) Revised effective ionic radii and systematic studies of interatomic distances in halides and calcogenides. *Acta Crystallogr.* **A32**, 751–67.

Starynkevitch, I. (1922) The chemical formula of monazite and several analyses of Russian monazites. *Doklady Akad. Nauk S.S.S.R.*, **31**, 28–30 (in Russian).

Taylor, M. and Ewing, R.C. (1978) The crystal structures of the $ThSiO_4$ polymorphs: huttonite and thorite. *Acta Crystallogr.*, **B34**, 1074–9.

Ueda, T. (1967) Reexamination of the crystal structure of monazite. *J. Jpn. Assoc. Mineral. Petrol. Econ. Geol.*, **58**, 170–9.

Vainshtein, E.E., Tugariniv, A.I. and Turanskaya, V.I. (1956) Regularities in the distribution of rare earths in certain minerals. *Geochemistry*, **2**, 159–78.

von Knorring, O. and Clifford, T.N. (1960) On a skarn monazite occurrence from the Namib desert near Usakos, South-West Africa. *Mineral. Mag.*, **32**, 650–3.

[*Manuscript received 20 June 1995: revised 5 March 1996*]